Tuijin Jishu/Journal of Propulsion Technology
ISSN: 1001-4055
Vol. 44 No. 4 (2023)

Heat and Mass Transfer on 3D MHD Flow of Casson Nanofluid in Presence of Arrhenius Activation Energy

Motamari Madhu[1*], [2* 3] Maddileti Pasupula

[1*]*Department of Mathematics, University College, Palamuru University, Mahabubnagar-509001, Telangana, India*

[2*, 3]*Departement of Mathematics, University College of Science and Informatics, Mahatma Gandhi Universitu, Nalgonda-508254, Telangana, India*

Abstract: **-**This work studied the influence of heat and mass transfer on the convective nanofluid motion of Casson nanofluid via linear stretched sheet. The main aim to analyse the characteristics of heat and mass transfer in Casson liquid under convective condition with effects of thermal radiation, heat generation and Arrhenius activation energy. We utilize some suitable similarity transformations to translate the governing PDEs and the initial boundary conditions of present model into a couple of nonlinear ODEs. We applied shooting procedure to solve the set of highly nonlinear ODEs numerically and calculate numerical results are related with those gained by the help of MATLAB bvp4c solver. The effect of prominent parameters of interest such as activation parameter, Lewis number, Thermophoresis parameter, Brownian motion parameter, thermal radiation, magnetic parameter, on velocity, temperature and heat and mass transfer is also encompassed. the numerical values obtained for defined through graphs and tables. The validation of present numerical work compared to previous work.

Keywords: *Non-Linear Thermal Radiation, Casson Fluid, Arrhenius Activation energy.*

1. Introduction

Casson fluids are characterized by their non-linear relationship between shear stress and shear rate. It behaves like a solid at low shear rates and require a certain critical stress (yield stress) to start flowing. As the shear rate increases beyond this critical point, they behave as shear-thinning liquids, with decreasing viscosity. Casson fluid behavior can be observed in a variety of everyday liquids, including tomato sauce, honey, soup, orange juice, and even human blood. These fluids exhibit a combination of solid-like and liquid-like behavior, which makes them suitable for various culinary, medical, and industrial applications. Casson fluids, particularly when modified with nanoparticles (Casson nanofluids), have gained significant attention in the field of medicine. This modeling helps in understanding circulatory phenomena in various parts of the human body, including the brain. Casson-type nanofluids are also used in other areas of biological and engineering sciences. Researchers use these models to analyze various physical and biological characteristics, such as flow behavior in microfluidic devices, drug delivery systems, and the behavior of biological fluids under different conditions. Suresh Kumar et al. **[1]** have studied the behavior of Casson nanofluid motion via exponentially stretching surface. Taj and

Salahuddin **[2]** examined the effect of viscous dissipation and nonlinear radiation in a three-dimensional Williamson fluid flow over an exponentially stretching surface. Mohamed Ibrahim and Fawzy **[3]** investigated Arrhenius activation energy in a rotating flow of Casson nanofluid. Wang et al. **[4]** studied the impact of activation energy on 3D nanofluid motion over a stretching surface. Ahmad Lone et al.**[5]** encountered the non-Newtonian Casson fluid's magnetohydrodynamic flow over a stratified extending sheet. Jana Reddy et al. **[6]** investigated the Casson nanofluid flow characteristics over a permeable stretched sheet. Wang et al. **[7]** examined the effects of activation energy and chemical reactions in non-Newtonian liquid flow over a stretching sheet. Suresh Kumar et al. **[8]** presented Brownian and thermophoresis effects with activation energy and nonlinear thermal radiation. Shah et al. **[9]** have examined the radiative electrically conducting Casson nanofluid flow over a nonlinearly stretching sheet in this study. Mahanta et al. **[10]** investigate irreversibility in a 3D MHD Casson nanofluid motion between two horizontal stretching surface. Tarakaramu et al. **[11]** examined the three-dimensional couple stress Casson fluid flow over a porous stretching sheet. Waqas et al. **[12]** examined the Falkner-Skan bioconvection flow of a cross nanofluid. Khan et al. **[13]** studied the movement of heat and mass in Oldroyd-B fluid flow over a rotating disk. Shankar Goud et al. **[14]** developed the magnetohydrodynamic Casson liquid motion via non-linear stretching surface. Riaz Khan et al. **[15]** explored radiated stagnation point motion of a time-dependent Casson fluid via permeable stretching/shrinking surface.

Activation energy is a fundamental concept in chemistry that affects various aspects of chemical reactions and processes across multiple industries. It helps scientists and engineers design and optimize reactions and systems for practical applications. Some applications are manufacturing of food items, geothermal repository, design of chemical production, oil emulsion formation, etc. Tarakaramu et al. **[16]** explored non-Newtonian nanofluid flow in three dimensions over a porous stretching sheet. Zeeshan et al. **[17]** evaluated various flow scenarios in applied sciences, particularly in areas like nuclear reactor cooling, geothermal reservoirs, chemical engineering, and thermal oil recovery. Khan et al. **[18]** examined the generation of entropy during the radiative spinning motion of a Casson nanofluid with Brownian and thermophoretic forces. Alrehili et al. **[19]** contributed many engineering applications by investigating the behavior of dissipative Carreau nanofluids flowing over nonlinearly stretching sheets, considering the influence of thermal radiation. Abideen and Saif **[20]** investigated heat transfer in a radiative nanofluid flowing over a curved surface. Ahmed et al. **[21]** developed bioconvective motion of hybrid nanoliquid via spinning disk with Arrhenius activation energy.Jawad et al. **[22]** explored Arrhenius activation energy on Darcy-Forchheimer motion of Maxwell nanofluid motion via porous stretching sheet. Puneeth et al. **[22]** presented bioconvection Jet motion of Williamson nanofluid in porous medium with effect of Arrhenius activation energy.

The motivation of present work, jet flow is indeed an effective method for enhancing heat and mass transfer in various industrial applications. Due to the higher coefficients of heat and mass transfer associated with jet flows compared to other methods of fluid flow. Further, the existence of magnetic field uses to controlling the velocity of Casson nanoliquid motion.

2. Mathematical Analysis

Consider 3D magnetohydrodynamic flow of a non-Newtonian nanofluid over a stretching sheet $z=0$ along xy-plane while fluid is located along with z-direction. The fluid flow region is taken as $z>0$. The velocity components $u_1 = ax$ and $u_2 = by$ along $x,\ y$- directions respectively as shown in **Fig. 1**. Moreover, it has taken that the constant Magnetic field is applied normal to the fluid flow direction and it is assumed that induced magnetic field is negligible. We considered that the rheological equation **[ref. 23]** of extra stress tensor τ for an isotropic and incompressible flow of a Casson fluid can be written as [**ref. 24**]:

$$\tau_{ij} = \begin{cases} 2e_{ij}\left(\mu_B + p_y\big/\sqrt{2\pi}\right), & \pi > \pi_c \\ 2e_{ij}\left(\mu_B + p_y\big/\sqrt{2\pi_c}\right), & \pi < \pi_c \end{cases}$$

Based on above construction we have to formulate the governing equations in the present flow analysis as (**ref. 23-27**):

$$\frac{\partial u_1}{\partial x^*} + \frac{\partial u_2}{\partial y^*} + \frac{\partial u_3}{\partial z^*} = 0 \tag{1}$$

$$u_1\frac{\partial u_1}{\partial x^*} + u_2\frac{\partial u_1}{\partial y^*} + u_3\frac{\partial u_1}{\partial z^*} = \upsilon^*\left(1+\beta^{-1}\right)\frac{\partial^2 u_1}{\partial z^{*2}} - \frac{\sigma^* B_0^2}{\rho^*}u_1 \tag{2}$$

$$u_1\frac{\partial u_2}{\partial x^*} + u_2\frac{\partial u_2}{\partial y^*} + u_3\frac{\partial u_2}{\partial z^*} = \upsilon^*\left(1+\beta^{-1}\right)\frac{\partial^2 u_2}{\partial z^{*2}} - \frac{\sigma^* B_0^2}{\rho^*}u_2 \tag{3}$$

$$u_1\frac{\partial T^*}{\partial x^*} + u_2\frac{\partial T^*}{\partial y^*} + u_3\frac{\partial T^*}{\partial z^*} = \alpha_m\frac{\partial^2 T^*}{\partial z^{*2}} + \varsigma\left(D_B\frac{\partial T^*}{\partial z^*}\frac{\partial C^*}{\partial z^*} + \frac{D_T}{T_\infty^*}\left(\frac{\partial T^*}{\partial z^*}\right)^2\right) - \frac{1}{(\rho^* C^*)_f}\frac{\partial q_r}{\partial z^*} - \frac{Q_0}{(\rho^* C^*)_f}(\mathrm{T}^* - \mathrm{T}_\infty^*) \tag{4}$$

$$u_1\frac{\partial C^*}{\partial x^*} + u_2\frac{\partial C^*}{\partial y^*} + u_3\frac{\partial C^*}{\partial z^*} = \left(D_B\frac{\partial^2 C^*}{\partial (z^*)^2} + {D_T}\big/{T_\infty^*}\frac{\partial^2 T^*}{\partial (z^*)^2}\right) - K_r^2\left(C^* - C_\infty^*\right)\left(\frac{T^*}{T_\infty^*}\right)^m \exp\left(\frac{-E_1 a_1}{k_1 T^*}\right)$$

(5)

The relevant boundary conditions of the present model as

$$\left.\begin{array}{lllll} u_1 = ax, & u_2 = by, & u_3 = 0, & -k\dfrac{\partial T^*}{\partial z} = h_1(\mathrm{T}_f^* - \mathrm{T}^*), \quad -D\left(\dfrac{\partial C^*}{\partial z}\right) = h_2\left(C_f^* - C^*\right) & \text{at} \quad \mathrm{z}^* = 0 \\ u_1 \to 0, & u_2 \to 0, & T^* \to T_\infty^*, & C^* \to C_\infty^* & as \quad z^* \to \infty \end{array}\right\}$$

(6)

The radiative heat flux q_r which is given by Quinn Brewster **[28]** is given by

$$\left. q_r = -\frac{4\sigma^*}{3K^*}\frac{\partial\left(T^*\right)^4}{\partial z} = -\frac{16\sigma^*}{3K^*}\left(T^*\right)^3\frac{\partial T^*}{\partial z}\right\}$$

(7)

Differentiate above heat flux equation, we get

$$\frac{\partial q_r}{\partial z}=-\frac{16\sigma^*}{3K^*}\frac{\partial}{\partial z}\left(\left(T^*\right)^3\frac{\partial T^*}{\partial z}\right)$$

(8)

Substituting **Eq. (8)** in **Eq. (4),** we get below Expression

$$\left.\begin{aligned}u_1\frac{\partial T^*}{\partial x}+u_2\frac{\partial T^*}{\partial y}+u_3\frac{\partial T^*}{\partial z}=\alpha_m\frac{\partial^2 T^*}{\partial z^2}+\frac{1}{(\rho^* C^*)_f}\left(\frac{16\sigma^*}{3K^*}\frac{\partial}{\partial z}\left(\left(T^*\right)^3\frac{\partial T^*}{\partial z}\right)\right)-\frac{Q_0}{(\rho^* C^*)_f}(\mathrm{T}^*-\mathrm{T}_\infty^*)\\+\frac{(\rho^* C^*)_p}{(\rho^* C^*)_f}\left(D_B\frac{\partial T^*}{\partial z}\frac{\partial C^*}{\partial z}+\frac{D_T}{T_\infty^*}\left(\frac{\partial T^*}{\partial z}\right)^2\right)\end{aligned}\right\}$$

(9)

The similarity transformations as below

$$\left.\begin{aligned}&\eta_1=\sqrt{\frac{a}{\upsilon^*}}z,\quad u_1=axf'(\eta),\qquad u_2=ayg'(\eta),\qquad u_3=-\sqrt{a\upsilon^*}\left(f(\eta)+g(\eta)\right)\\&\theta(\eta)=\frac{T^*-T_\infty^*}{T_w^*-T_\infty^*},\qquad \phi(\eta)=\frac{C^*-C_\infty^*}{C_w^*-C_\infty^*}\end{aligned}\right\}(10)$$

Using above **Eq. (10)**, we are converting **Eq. (2)-(4)** and **Eq. (9)** into below format

$$f'''\left(1+\frac{1}{\beta}\right)+f''(f+\mathrm{g})-(f')^2-Mf'=0$$

(11)

$$\mathrm{g}'''\left(1+\frac{1}{\beta}\right)+g''(f+\mathrm{g})-(g)^2-Mg'=0$$

(12)

$$\left(\left(1+R_d\left(\theta(\theta_w-1)+1\right)^3\right)\theta'\right)'+\Pr\left((f+\mathrm{g})\theta'+N_b\theta'\phi'+\mathrm{N}_t\,\theta'^2\right)+H\theta=0$$

(13)

$$\phi''+Le(f+\mathrm{g})\phi'+\frac{N_t}{N_b}\theta''-Le\delta\left(1+R\theta\right)^r e^{\left(-E/_{1+R\theta}\right)}=0$$

(14)

Corresponding boundary conditions as below

$$\left.\begin{aligned}&f=0,\quad g=0,\quad f'=1,\quad g'=\lambda,\quad \theta'=-Bi_t(1-\theta),\quad \phi'=-Bi_c(1-\phi)\ \ at\ \eta_1=0\\&f'\to 0,\ \ g'\to 0,\ \ \theta\to 0,\ \ \phi\to 0,\qquad\qquad\qquad\qquad\qquad as\ \ \eta_1\to\infty\end{aligned}\right\}(15)$$

Moreover, the skin-friction coefficient and Nusselt number are below

$$\left.\begin{array}{ll}(\mathrm{Re}_x)^{1/2}C_{fx} = (1+\beta^{-1})\,f''(0), & (\mathrm{Re}_x)^{1/2}C_{fy} = (1+\beta^{-1})g''(0)\\ (\mathrm{Re}_x)^{-1/2}Nu_x = -(1+R_d(\theta(\theta_w-1)+1)^3)\,\theta'(0), & \mathrm{Sh}_x\mathrm{Re}_x^{-1/2} = -\phi'(0)\end{array}\right\}(16)$$

3. Results and Discussion

The characteristics of M (Magnetic Parameter), β (Casson Parameter) on $g'(\eta_1)$ (Transverse Direction) represented in **Figs. 2(a)-2(b)**,respectively. It is found that, the velocity of Casson liquid motion declined with higher enhanced values of magnetic parameter, Casson parameter respectively. Physically, the Lorenze force applied into opposite direction to the liquid motion then liquid velocity should go slowly in transverse surface.

The physical impact of Pr (Prandtl number) on $\theta(\eta_1)$ (Temperature Profile) predicted in **Figs. 3**. It is has seen that, the temperature declined with large numerical values of Pr. Physically, the Prandtl number is interrelated between thermal viscosity and thermal diffusivity. Due to high efficiency of thermal viscosity reduces to temperature of Casson nanoliquid motion on stretching surface.

The physical impact of Bi_t (Temperature Biot number) on $\theta(\eta_1)$ (Temperature Profile) predicted in **Figs. 4**. It is has seen that, the temperature enhanced with large numerical values of Bi_t. Physically, the temperature Biot number is reciprocal of thermal conductivity, due to high efficiency of thermal conductivity produced more temperature of Casson nanoliquid motion on stretching surface.

The physical impact of H (Temperature Biot number), R_d (Thermal Radiation) on $\theta(\eta_1)$ (Temperature Profile) predicted in **Figs. 5(a)-5(b)**. It perceived that, the temperature declined with enlarge numerical values of H while reverse trend behaviour of R_d (Thermal Radiation), respectively. Physically, the high efficiency of thermal conductivity produced more temperature of Casson nanoliquid motion on stretching surface.

The physical impact of N_b (Brownian Motion Parameter), N_t (Thermophoresis Parameter) on $\theta(\eta_1)$ display in **Figs. 6(a)-6(b)**. It perceived that, the temperature enhanced more in Casson liquid for higher numerical values of N_b, N_t. Physically, the high efficiency of thermal diffusivity applied to liquid particles of Casson nanoliquid clashes between each particle in liquid motion produced more temperature in Casson nanoliquid at stretching surface area.

Fig. 7 shows E (Arrhenius Activation Energy) on $\phi(\eta_1)$. It perceived that, the Concentration has high in Casson nanoliquid for higher numerical values of E, but the boundary layer moves very low convergence. Physically, the high efficiency of thermal conductivity applied in Casson nanoliquid motion produced more concentration at stretching surface.

Fig. 8 shows Le (Lewis Number) on $\phi(\eta_1)$. It perceived that, the Concentration has high and reverse behaviour of mass transfer rate in Casson nanoliquid for higher numerical values of Le as shown in **Fig.9,** but the boundary layer moves very high efficiency. Physically, the high efficiency of thermal diffusivity of Casson nanoliquid motion produced more concentration at stretching surface.

The physical parameter of thermal radiation over thermophoresis parameter on heat transfer rate as predicted in **Fig.10**.It is clear that, the heat transfer rate is high for enlarge values of thermal radiation.

4. Conclusion

The main out comes of present work as follows

- The heat transfer rate is high with large numerical values of nonlinear thermal radiation.
- The mass transfer rate is declined with enhanced numerical values of Lewis number.
- The temperature is high efficiency for large number of values of E and Le.

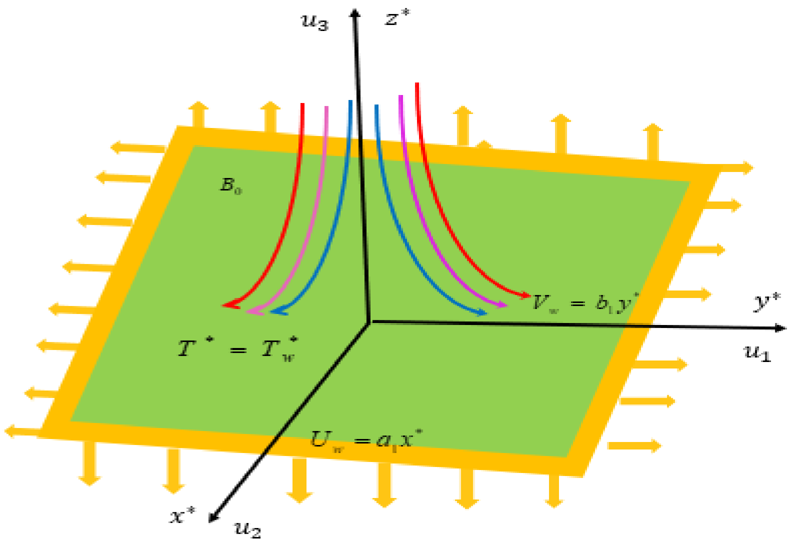

Fig. 1 Physical geometry of the problem

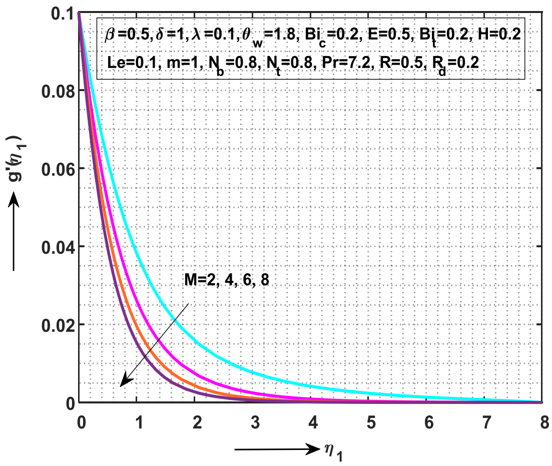

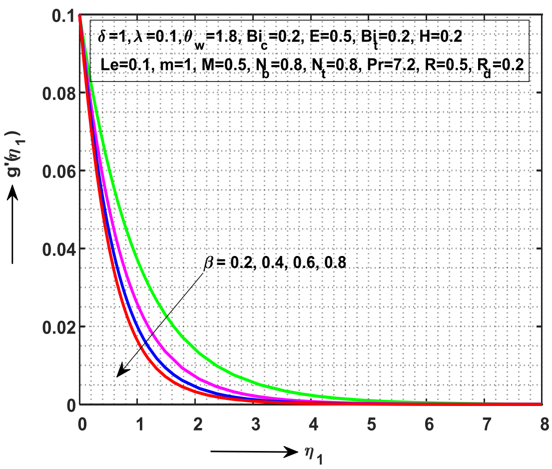

Fig. 2(a) Impact of M on $g'(\eta_1)$ Fig. 2(b) Impact of β on $g'(\eta_1)$

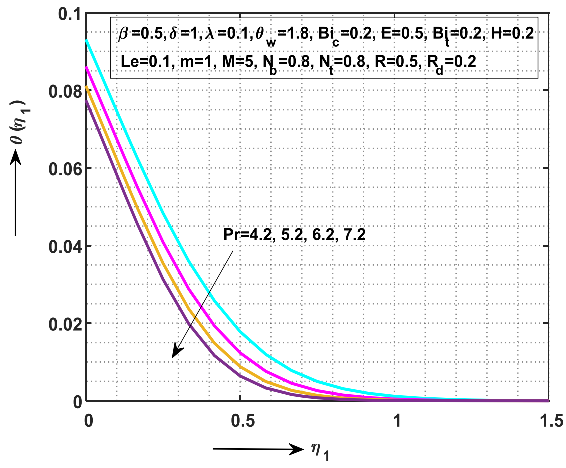

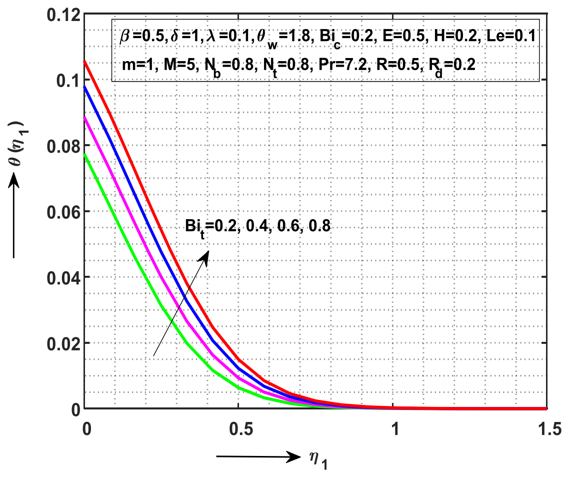

Fig. 3 Impact of $\Pr$ on $\theta(\eta_1)$ **Fig. 4** Impact of Bi_t on $\theta(\eta_1)$

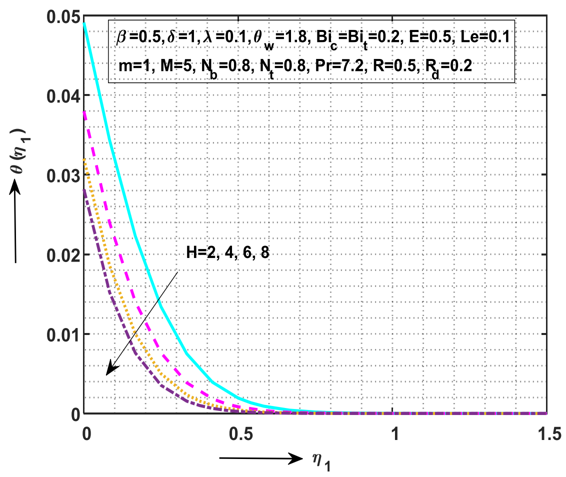

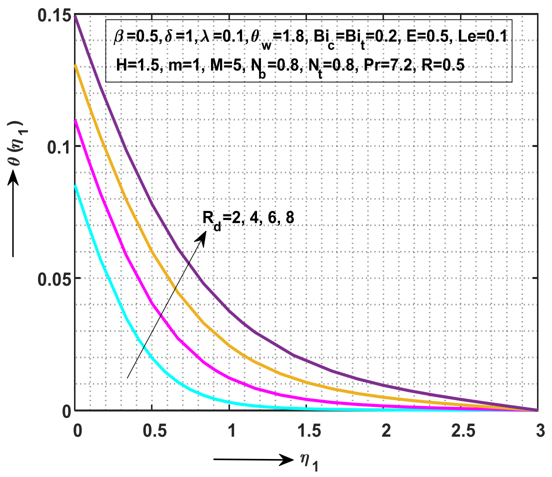

Fig. 5(a) Impact of H on $\theta(\eta_1)$ **Fig. 5(b)** Impact of R_d on $\theta(\eta_1)$

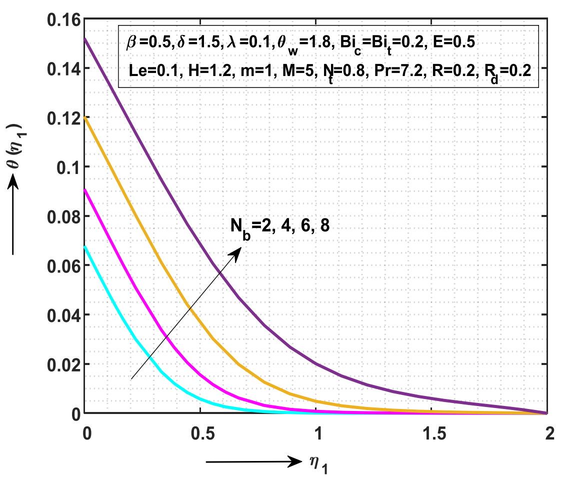

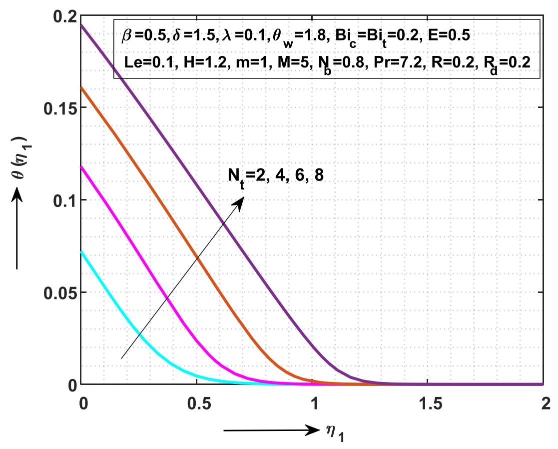

Fig. 6(a) Impact of N_b **on** $\theta(\eta_1)$ **Fig. 6(b) Impact of** N_t **on** $\theta(\eta_1)$

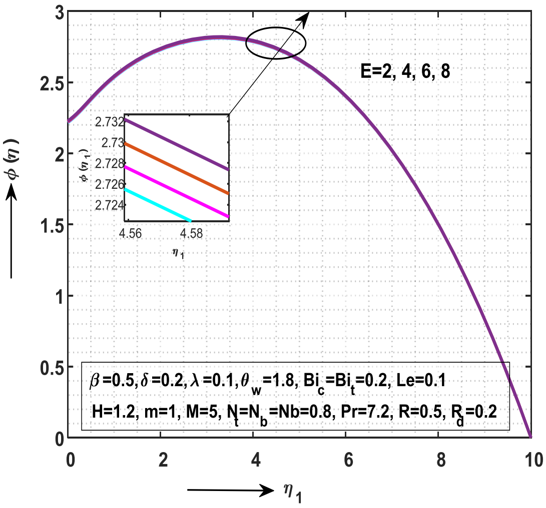

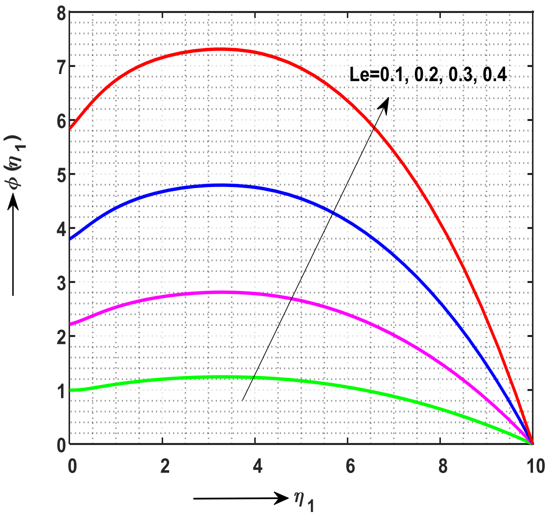

Fig. 7 Impact of E **on** $\phi(\eta_1)$ **Fig. 8 Impact of** Le **on** $\phi(\eta_1)$

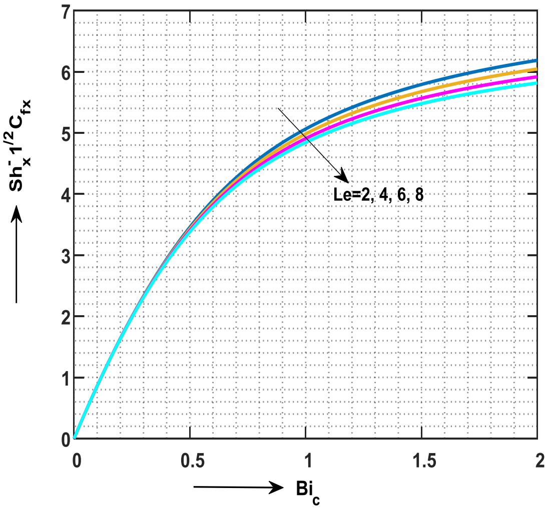

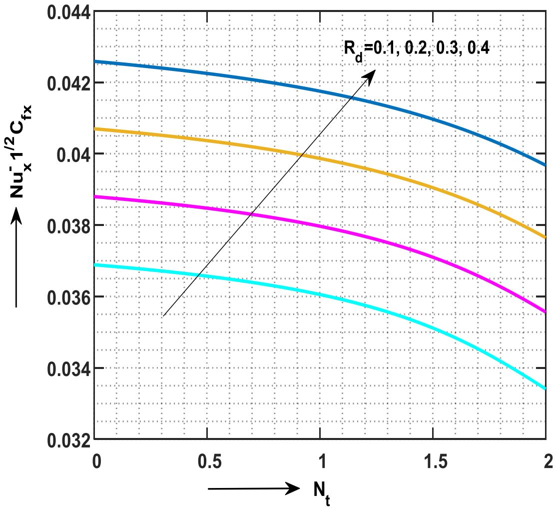

Fig. 9 Impact of Le on $Sh_x^{-0.5}C_{fx}$ **Fig. 10** Impact of R_d on $Nu_x^{-0.5}C_{fx}$

Table. 1 Evaluation of Skin friction coefficient $\left(1+\beta^{-1}\right)f''(0)$, $\left(1+\beta^{-1}\right)g''(0)$ **for various values** λ **.**

λ	**Wang [29]** $-f''(0)$	**Present study** $-f''(0)$	**Wang [29]** $-g''(0)$	**Present study** $-g''(0)$
0.00	1.0000	1.00000	0.0000	0.00000
0.20		1.03949		0.14873
0.25	1.0488	1.04881	0.1945	0.19456
0.40		1.07578		0.34921

0.50	1.0930	1.09309	0.4652	0.46520
0.60		1.10994		0.59053
0.75	1.1344	1.13448	0.7946	0.79462
0.80		1.14248		0.86668
1.00	1.1737	1.17372	1.1737	1.17372

Table. 2 Comparison of Skin friction coefficient for $\beta \to \infty$ and various values of λ

λ	**Wang [29]** $f(\infty)$	**Present study** $f(\infty)$	**Wang [29]** $g(\infty)$	**Present study** $g(\infty)$
0.00	1.0000	1.00000	0.0000	0.00000
0.20		0.92265		0.23236
0.25	0.9070	0.90707	0.2579	0.25798
0.40		0.86603		0.37922
0.50	0.8423	0.84236	0.4516	0.45167
0.60		0.82096		0.51896
0.75	0.7923	0.79230	0.6120	0.61212
0.80		0.78350		0.64143
1.00	0.7515	0.75152	0.7515	0.75148

Refrences

[1] Y. Suresh Kumar, S. Hussain, K. Raghunath, F. Ali, K. Guedri, M. Sayed Eldin and M. Ijaz Khan M, Numerical analysis of magnetohydrodynamics Casson nanofluid flow with activation energy, Hall current and thermal radiation, Scientific Reports, 13 (2023). Https://doi.org/10.1038/s41598-023-28379-5.

[2] M. Taj, and T. Salahuddin, Analysis of viscously dissipated three-dimensional flow of Williamson fluid with nonlinear radiation and activation energy, Alexandria Engineering Journal, 76(1) (2023) 595-607.

[3] G. Mohamed Ibrahim and Fawzy, Arrhenius energy effect on the rotating flow of Casson nanofluid with convective conditions and velocity slip effects: Semi-numerical calculations, Heat Transfer, 52(1) (2023) 687-706.

[4] F. Wang, N. Tarakaramu, N. Sivakumar, P.V. Sathya Narayana, D. Harish Babu, and R. Sivajothi, Three dimensional nanofluid motion with convective boundary condition in presents of nonlinear thermal radiation via stretching sheet, Journal of the Indian Chemical Society, 100(2) (2023) 100882.

[5] S. Ahmad Lone, S. Anwar, A. Saeed and G. Bognár, A stratified flow of a non-Newtonian Casson fluid comprising microorganisms on a stretching sheet with activation energy, Scientific Reports, 13 (2023) 11240. https://doi.org/10.1038 /s41598-023-38260-0.

[6] S. Jana Reddy, P. Valsamy and D. Srinivas Reddy, Numerical Solutions of Casson-Nano Fluid Flow Past an Isothermal Permeable Stretching Sheet: MHD, Thermal Radiation and Transpiration Effects, Journal of Nanofluids, 12(6) (2023) 1503-1511(9).

[7] F. Wang, N. Tarakaramu, M.V. Govindaraju, N. Sivakumar and K. Bhagya Lakshmi, P.V. Satya Narayana, and R. Sivajothi, Activation energy on three-dimensional Casson nanofluid motion via stretching sheet: Implementation of Buongiorno's model, Journal of the Indian Chemical Society, 100(2) (2023) 100886.

[8] Y. Suresh Kumar, Y. Madhavi Reddy, M. Siva Mala and P. Srinivasa Rao,Effects of Activation Energy Diffusion Thermo and Nonlinear Thermal Radiation on Mixed Convection Casson Fluid Flow Through a Vertical Cone with Porous Media in the Presence of Brownian Motion and Thermophoresis,Journal of Advanced Research in Fluid Mechanics and Thermal Sciences, 12(1) (2023) 147-156.

[9] Z. Shah, P. Kumam and W. Deebani, Radiative MHD Casson Nanofluid Flow with Activation energy and chemical reaction over past nonlinearly stretching surface through Entropy generation, Scientific Reports, 10, 4402 (2020).

[10] G. Mahanta, M. Das, M.K. Nayak and S. Shaw S, Irreversibility Analysis of 3D Magnetohydrodynamic Casson Nanofluid Flow Past Through Two Bi-Directional Stretching Surfaces with Nonlinear Radiation, Journal of Nanofluids, (2021). doi:10.1166/jon.2021.1793.

[11] N. Tarakaramu, P.V. Satya Narayana, R. Sivajothi, K. Bhagya Lakshmi D. Harish Babu and B. Venkateswarlu, Three- dimensional non- Newtonian couple stress fluid flow over a permeable stretching surface with nonlinear thermal radiation and heat source effects, Heat Transfer, (2021). DOI: 10.1002/htj.22550.

[12] H. Waqas, S. Ali Khan, S.U. Khan, M. Ijaz Khan, K. Seifedine, C. Yu-Ming, Falkner-Skan time-dependent bioconvection flow of cross nanofluid with nonlinear thermal radiation, activation energy and melting process, International Communications in Heat and Mass Transfer, (2021). https://doI.org/10.1016 /j. Icheatmasstrans fer.2020.105028.

[13] M. Khan, A. Hafeez and J. Ahmed, Impacts of non-linear radiation and activation energy on the axisymmetric rotating flow of Oldroyd-B fluid, Physica A: Statistical Mechanics and its Applications, (2021). https://doI.org/10 .1016/j.physa .2019. 124085.

[14] B. Shankar Goud, Y. Dharmendar Reddy, J. Wasim, N. Kottakkaran Sooppy, N.A. Abdulaziz and C. Ridha, Radiation eff ect on MHD Casson fluid flow over an inclined non-linear surface with chemical reaction in a Forchheimer porous medium, Alexandria Engineering Journal, (2022). https://doI.org /10.1016/j.aej.2022.01.043.

[15] M. Riaz Khan, A.S. Al-Johani, M.A.E. Awatif, S. Tareq, A.A. Abd, The computational study of heat transfer and friction drag in an unsteady MHD radiated Casson fluid flow across a stretching/shrinking surface, International Communications in Heat and Mass Transfer, (2022). https:/doi.org/101016/j. icheatmasstransfer.2021.105832.

[16] N. Tarakaramu, P.V. Satya Narayana, N. Sivakumar, D. Harish Babu, K. Bhagya Lakshmi, (2023). Convective Conditions on 3D Magnetohydrodynamic (MHD) Non-Newtonian Nanofluid Flow with Nonlinear Thermal Radiation and Heat Absorption: A Numerical Analysis, Journal of Nanofluids, http://dx.doI.org/10 .1166/jon.2023.1939.

[17] A. Zeeshan, M. Obaid Ullah, M. Fazle, A. Faris, Numerical analysis of hydromagnetic transport of Casson nanofluid over permeable linearly stretched cylinder with Arrhenius activation energy, International Communications in Heat and Mass Transfer, 130 (2021) 105736.

[18] A. Khan, Z. Shah and E. Alzahrani and S. Islam, Entropy generation and thermal analysis for rotary motion of hydromagnetic Casson nanofluid past a rotating cylinder with Joule heating effect, International Communications in Heat and Mass Transfer, 119 (2023) 104979. https://doi.org/10.1016/j.Icheatmass transfer.2020.104979.

[19] M. Alrehili, Improvement for engineering applications through a dissipative Carreau nanofluid fluid flow due to a nonlinearly stretching sheet with thermal radiation, Case Studies in Thermal Engineering, 42 (2023). https://doi.org/10.1016 /j. csite.2023.102768.

[20] Z.U. Abideen and R.S. Saif, Impact of thermal radiation and internal heat generation on Casson nano-fluid flowing by a curved stretchable surface with suspension of carbon nanotubes, Heliyon, 9(8) (2023) e18941.

[21] S. E. Ahmed, A.A. M. Arafa and S.A. Hussein, Bioconvective flow of a variable Properties hybrid nanofluid over a spinning disk with Arrhenius activation energy, Soret and Dufour impacts, Numerical Heat Transfer, Part A: Applications, (2023). https://doi.org/10.1080/10407782.2023.2193709.

[22] M. Jawad, H. Maria Kirn, K. Sooppy Nisar and A. Hussain Majeed, Darcy-Forchheimer flow of maxwell nanofluid flow over a porous stretching sheet with Arrhenius activation energy and nield boundary conditions, Case Studies in Thermal Engineering, 44 (2023) 102830.

[23] V. Puneeth, S. Manjunatha, M. Shoaib Anwar, M. Oreijah, K. Geudri, O.T. Bafakeeh and A.M. Galal, Stratified Bioconvective Jet Flow of Williamson Nanofluid in Porous Medium in the Presence of Arrhenius Activation Energy, Journal of Computational Biophysics and Chemistry, 22(3) (2023) 209-319.

[24] S. Gupta and K. Sharma, Numerical simulation for magnetohydrodynamic three-dimensional flow of Casson nanofluid with convective boundary conditions and thermal radiation. Engineering Computations (2017) 1-32.

[25] K. Bhattacharyya, T. Hayat and A. Alsaedi, Exact solution for boundary layer flow of Casson fluid over a permeable stretching/shrinking sheet. ZAMM-Z. Angew. Math. Mech. (2013) 1-7. DOI:10.1002/zamm.201200031.

[26] M. Nakamura and T. Sawada, Numerical study on the flow of a non-Newtonian fluid through an axisymmetric stenosis. Journal Biomechanical Engineering 110(137) (1988) 1-7.

[27] M. Nakamura and T. Sawada, Numerical study of the lamina pulsatile flow of slurries. Journal Non-Newtonian Fluid Mechanics 22 (1987) 191-206.

[28] M. Q. Brewster, Thermal radiative transfer properties, Wiley, New York, 1972.

[29] C. Y. Wang, The three-dimensional flow due to a stretching flat surface, Phys. Fluids 27 (1915) (1984) 1-4. Doi: 10.1063/1.864868.

Nomenclature			
(x^*, y^*, z^*)	Cartesian coordinate's	Sc	Schmidt number $= \upsilon_f^* / D_B$
u_1, u_2, u_3	velocity components along (x^*, y^*, z^*) axis	T_w^*	Convection fluid temperature at wall
C^*	volume fraction of nanoparticle	T^*	Temperature of the fluid (K)
C_f^*	Skin friction coefficient	T_∞^*	fluid temperature far away from the surface
c_p^*	Specific heat $(kJ/kg\ K)$	V_w	Stretching velocity at y-direction
C_∞^*	Uniform ambient concentration (kgm^{-3})	U_w	Stretching velocity at x-direction
C_w^*	Convective fluid concentration (kgm^{-3})		***Greek symbols***
D_B	Brownian diffusion	α_m	Thermal diffusivity $= k/(\rho c_p)_f$ $(m^2 s^{-1})$
D_T	Thermophoresis diffusion $(m^2.s^{-1})$	μ	Dynamic viscosity $(Pa.s^{-1})$
f	Dimensionless stream function	ϕ	Dimensionless concentration
f'	Dimensionless velocity	σ^*	Boltzmann Stefan constant $(wm^2 s^{-1} K^{-4})$
h_1	Convection heat transfer coefficient	σ	Electrical conductivity
h_2	Convection mass transfer coefficient	β	Casson fluid parameter
H	Heat absorption parameter $\frac{Q_0 (T^* - T_\infty^*)}{(\rho^* C^*)_f}$	υ^*	Kinematic viscosity $(m^2 s^{-1})$

k^* Mean absorption coefficient	θ Dimensionless temperature
k Thermal conductivity	λ Stretching parameter b/a
	ρ_f Fluid density $\left(Kg.s^{-1}\right)$
M Magnetic field parameter $=\dfrac{\sigma^* B_0^2}{a\rho_f^*}$	ς Ratio of the nanoparticle heat capacity and base fluid heat capacity $\left(\rho^* C^*\right)_p / \left(\rho^* C^*\right)_f$
N_b Brownian motion coefficient $=\dfrac{D_B\,\varsigma(C_w^*-C_\infty^*)}{\upsilon_f^*}$	Bi_t Temperature Biot number $= h_1/k\,\sqrt{\upsilon^*/a}$
N_t Thermophoresis parameter $=\dfrac{\varsigma D_T}{\upsilon_f^*\,T_\infty^*}(T_w^*-T_\infty^*)$	Bi_c Concentration Biot number $= h_1/k\,\sqrt{\upsilon^*/a}$
Pr Prandtl number $=\left(\dfrac{\upsilon_f^*}{\alpha_m}\right)$	$\left(\rho^* C^*\right)_p$ Heat capacity of the nanoparticle to the fluid $\left(Jm^3K\right)$
Re_x Reynolds number	$\left(\rho^* C^*\right)_f$ Heat capacity of the fluid $\left(kJ\,kg^{-1}\right)$
q_r Radiative heat flux $\left(Wm^{-2}\right)$	***Subscripts***
R_d Radiation parameter $=\dfrac{16\sigma^* T^{*3}}{3\alpha_m k k^*}$	∞ condition at free stream